Journal of Power Sources, *20* (1987) 53 - 59

PROPERTIES OF LiCl LAYERS FORMED ON LITHIUM IN VARIOUS $SOCl_2$ SOLUTIONS

M. MOGENSEN

Metallurgy Department, Risø National Laboratory, DK-4000 Roskilde (Denmark)

Summary

The growth rate of LiCl solid electrolyte layers on Li was studied in neutral and acid $LiAlCl_4$–$SOCl_2$ solutions over periods of years. For SO_2-containing acid solutions, a small anodic load resulting from the coupling of lithium to stainless steel proved to be more important than the acidity.

The ionic and electronic conductivities of the layers were derived from impedance measurements and passivation rates, respectively. In neutral solutions, the Li^+ conductivity decreased with increase in the layer thickness; this effect was not observed in acid SO_2-containing solutions.

Factors influencing the growth rate of the LiCl layer are briefly analysed. It is concluded that increasing the ratio of ionic to electronic conductivity would be the most efficient way of improving the performance of the solid electrolyte.

Introduction

When a lithium electrode is exposed to thionyl chloride solutions, a thin layer of insoluble LiCl is formed spontaneously. This layer acts as the solid electrolyte in Li–$SOCl_2$ batteries; it is often referred to as the solid electrolyte interphase (SEI).

The properties of the SEI to a large extent determine the performance of the Li–$SOCl_2$ battery. The internal cell resistance is approximately equal to the SEI resistance, and the unintentional growth of the LiCl layer causes the well known delayed voltage phenomenon. The corrosion rate of the lithium, *i.e.*, during the shelf life of the cell, is also determined by the properties of the SEI.

In most other lithium batteries, a reaction layer is also formed on the lithium electrode. As a consequence, considerable effort is being devoted to an investigation of the solid electrolyte layers formed *in situ* [1, 2].

Experimental

Lithium electrodes exposed to $SOCl_2$ solutions were characterized by means of a.c. impedance spectroscopy in a three electrode setup. In all cases,

0378-7753/87/$3.50

lithium was used for the reference electrodes. By using this arrangement, the impedance of the isolated SEI can be determined directly [3 - 5]. The impedance spectra generally covered the frequency range from 1 Hz to 20 000 Hz. A Solartron 1250 Impedance Analyser was used. In a few cases, measurements were made down to 10^{-3} Hz.

The development of the SEI impedance with time was followed in three types of $SOCl_2$ solutions:

I: 1.8 M $LiAlCl_4$
II: 1.2 M $LiAlCl_4$ + 0.6 M $AlCl_3$
III: 1.2 M $LiAlCl_4$ + 0.6 M $AlCl_3$ + 0.6 M SO_2

Type I is the neutral catholyte used in common Li–$SOCl_2$ batteries. Type II is acid and able to dissolve LiCl until all the Lewis acid ($AlCl_3$) is consumed by the reaction:

$$LiCl\ (insol.) + AlCl_3\ (sol.) \longrightarrow LiAlCl_4\ (sol.).$$

Type III is a weakly acid catholyte. The weak Lewis base, SO_2, neutralizes the $AlCl_3$ to some extent, causing a lower dissolution rate of LiCl than in type II [6].

In a single case, a cell was opened after one year, and the LiCl layer was examined using scanning electron microscopy (SEM).

Results

Passivation rate

Impedance spectra were measured at regular periods. From an impedance spectrum, the resistance of the SEI was derived as the difference between the high frequency and the low frequency intercepts between the depressed semi-circle and the real axis in the complex impedance plot. In the type III solution, two depressed semi-circles were observed in the impedance plot: a large one in the frequency range above 10 Hz; and a small one below 10 Hz [5]. The latter has been ignored in this context. The resistance increase rate, or passivation rate, is obtained by plotting SEI resistance *versus* time. Such plots are shown in Fig. 1 for lithium electrodes on glass in solutions of types I, II and III. The passivation rate of lithium coupled to stainless steel in type III solution is also shown.

Compared with type I, the type III solution strongly retarded the growth of the SEI over a period of 10 - 20 days. Afterwards, the resistance of the SEI increased very rapidly and reached the level of the SEI formed in the type I electrolyte after a couple of months. This fast increase could be suppressed for periods of years when a weak anodic load was imposed on the lithium by connecting the electrode to stainless steel. (Note, when stainless steel is exposed to the $SOCl_2$, it acts as a poor cathode.) This observation indicates that the effect of adding SO_2 to an acid catholyte is not entirely a matter of decreasing the dissolution rate of the LiCl layer compared with that of a type II solution. Probably the structure, and possibly also the com-

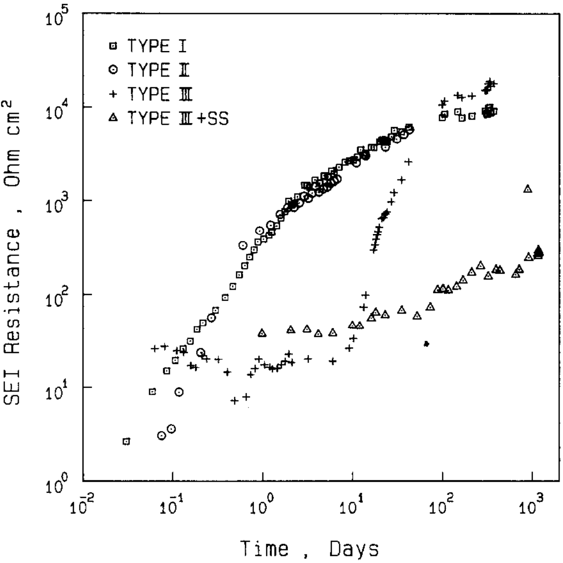

Fig. 1. Log–log plot of SEI resistance *vs.* exposure time of lithium electrodes on glass in the three solution types, and of lithium coupled to stainless steel (SS) in type III solution.

position of the layer, is affected. This is further supported by the difference in appearance of the complex impedance plots of types I and III solutions.

Coupling lithium to stainless steel in type I solution has been previously reported [5] to affect the passivation rate. After one day, the lithium coupled to stainless steel was less passive but afterwards the passivation rate was higher compared with lithium on glass. This again supports the basic differences between types I and III solutions.

In the acid type II solution, the growth of the SEI was retarded for a few hours and then the SEI growth rate and the properties were almost identical with the SEI on lithium in neutral type I solution. The interpretation of this is that the SEI in type II solution is initially very thin and this results in rapid corrosion. After a few hours, the $AlCl_3$ is neutralized by the LiCl formed by the corrosion process and the type II catholyte is thus converted to type I.

Appearance of the SEI

Figure 2 shows an electron micrograph of a lithium electrode surface taken after exposure for one year to type I solution. A very uneven surface is observed with small and large LiCl crystals. The apparent thickness was found to be about 5 - 10 μm, with heaps of crystals of about 100 μm size, one of which is shown in Fig. 2. The heaps had a spacing of a few mm between them. Figure 2 also shows a number of large and small cracks. Some of the cracks may be created during preparation, but other experiments [4] have indicated spontaneous crack formation during the SEI growth.

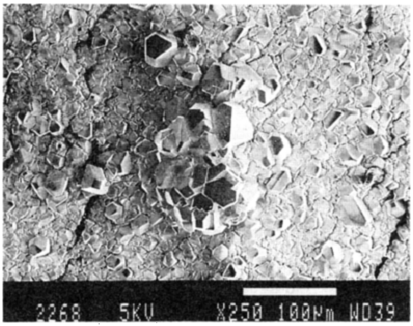

Fig. 2. Electron micrograph of a lithium electrode surface after one year of exposure. The heap of crystals and the many cracks are common features of the LiCl layer.

SEI conductivity

From the SEI admittance (inverse impedance), the specific conductivity (σ) and the relative electrical permittivity (ϵ_r) can be calculated from the formulae:

$$\sigma = \frac{dY'}{A} \tag{1}$$

$$\epsilon_r = \frac{dY''}{2\pi f \epsilon_0 A} \tag{2}$$

where Y' and Y'' are the real and the imaginary parts of the complex admittance, d is the SEI thickness, A is the exposed electrode area, f is the frequency, and ϵ_0 ($= 8.85 \times 10^{-14}$ F cm^{-1}) is the permittivity of the vacuum. The thickness, d, of the SEI must be determined in order to find σ and ϵ_r. At high frequency (~170 kHz), ϵ_r of LiCl is known from the literature to be about 11 (*i.e.*, 10.62 [7] and 11.05 [8]). Thus, d can be found from eqn. (2).

Figure 3 shows the SEI conductivity *versus* frequency, and Fig. 4 the SEI relative permittivity *versus* frequency, both in double logarithmic plots.

Both ϵ_r and σ are seen to be frequency dependent. It is noted that thicknesses calculated from eqn. (2) will only give approximate values because of the frequency dependency of ϵ_r, and the fact that frequencies above 20 kHz were not included in the present work.

Using Y'' at 20 kHz and $\epsilon_r = 11$, the SEI thickness was found to be about 10 nm and 600 nm after 1 h and one year of exposure, respectively. This average, or effective, thickness is an order of magnitude lower than the apparent thickness found in SEM studies. This also supports the conclusion that deep cracks are present in the SEI.

The conductivity derived from eqn. (1) is the Li^+ ionic conductivity, which is orders of magnitude above the electronic conductivity (see below). Figure 5 shows the variation in σ (Li^+) with average thickness for two different electrodes. The slopes of the curves in the log–log plots are about —0.8. At first, it was thought that this was due to a variation in space charge

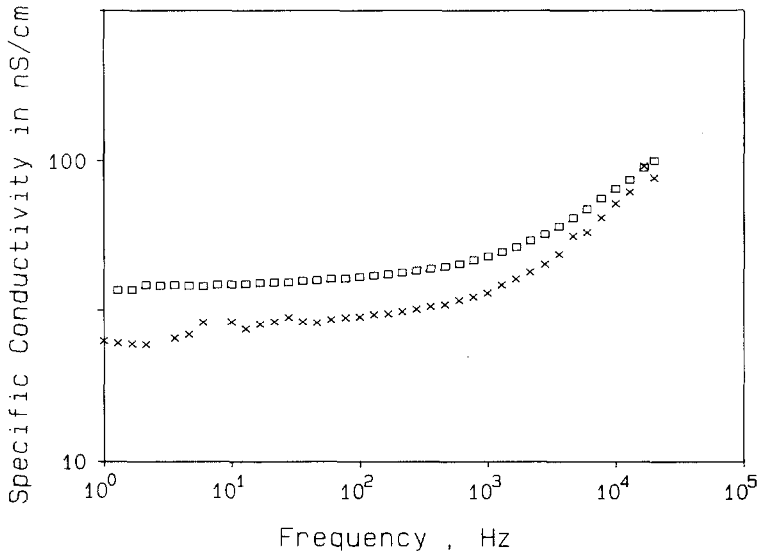

Fig. 3. Log–log plot of relative permittivity of the SEI *vs.* frequency. A relative permittivity of 11 was assumed at 20 kHz. Squares are for type I and crosses are for type III solutions.

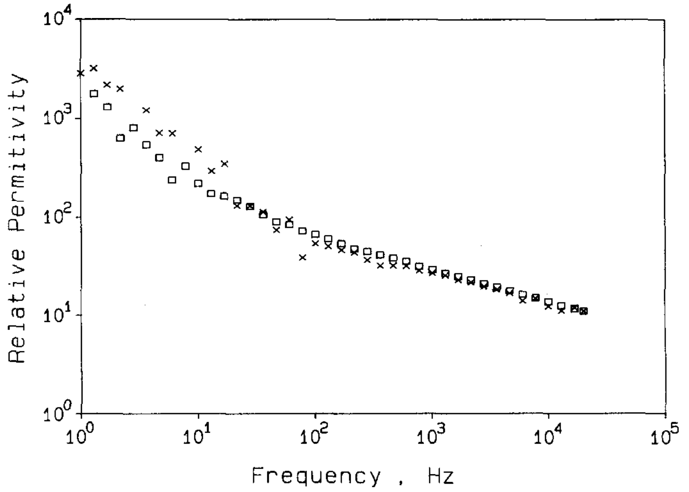

Fig. 4. Log–log plot of specific Li^+ conductivity *vs.* frequency. Squares are in type I, and crosses in type III solutions.

(= variation in Li^+ vacancies) with thickness. The space charge is expected to be significant in the thin SEI because of the large potential difference across the layer (equal to the cell voltage of 3.7 V). However, the phenomenon was observed only in the type I solution. Thus, if the space charge explanation holds, then an explanation of why the effect is only found in type I solutions is needed, but is not available.

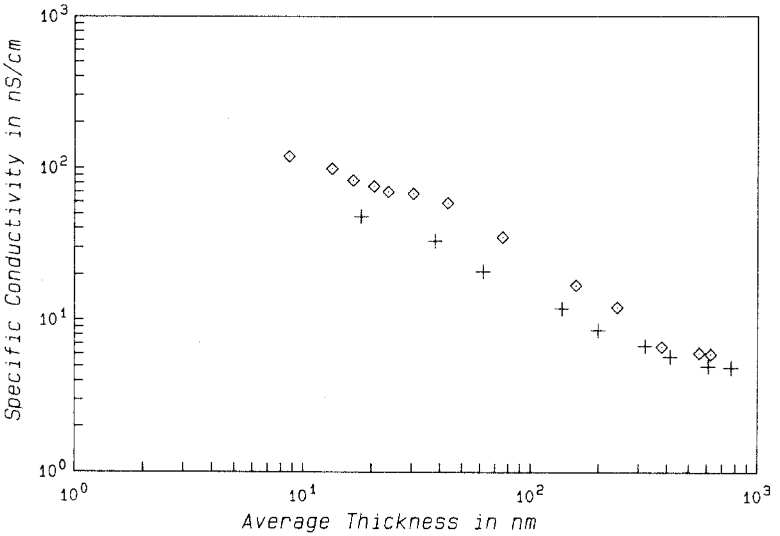

Fig. 5. Log–log plot of specific Li^+ conductivity of the SEI *vs.* average thickness for two electrodes in type I solution.

In the neutral type I solution, the SEI growth rate usually follows the parabolic law (slope 0.5 in Fig. 1) for some intermediate period. During this period, the SEI growth is controlled by electronic conductivity, σ_e, which can be estimated, as explained in ref. 3, from the formula:

$$\sigma_e = \frac{(d_2^2 - d_1^2)F}{2\Delta V V_m (t_2 - t_1)} \tag{3}$$

where d_1 and d_2 are the SEI thicknesses at times t_1 and t_2, respectively; F is the Faraday number; $\Delta V = (3.7\ \text{V})$ is the voltage across the SEI; and V_m (= 20.5 $\text{cm}^3\ \text{mol}^{-1}$) is the LiCl molar volume. By this method it was found that the electronic conductivity was about 3×10^{-3} nS/cm and 5×10^{-4} nS/cm for the two SEIs given in Fig. 5. The one with the smallest electronic conductivity has the largest Li^+ conductivity. The two experiments were nominally identical. The differences observed are thought to be due to small differences in the impurity level and/or composition.

Discussion

Problem analysis

As already mentioned, the SEI resistance determines the cell performance. Consequently, it is important to analyse the inter-relationships between the above measured parameters and observations.

The SEI resistance is equal to the *thickness* divided by *the specific Li^+ conductivity*. The *thickness* of the SEI obtained after a given exposure time is a result of:

(i) LiCl formation rate which is inversely proportional to the SEI thickness and directly proportional to its *specific electronic conductivity*;

(ii) dissolution rate of LiCl;

(iii) reprecipitation rate of LiCl;

(iv) morphology of precipitated LiCl.

It is generally known that the *specific* Li^+ *conductivity* of the LiCl is proportional to the concentration of higher valent ions such as Al^{3+} and Mg^{2+}. Furthermore, it is found here to be dependent on the LiCl layer thickness.

The *specific electronic conductivity* of ionic compounds increases with the concentration of transition metal ions with easily changeable valency, *e.g.*, Fe^{2+} and Fe^{3+}.

Problem solution

In future, the object of improving the performance of the SEI of LiCl should be pursued by trying to find means for:

(i) increasing the ratio of Li^+ conductivity to electronic conductivity (note, the ratio is important, not the absolute values);

(ii) decreasing the LiCl reprecipitation rate.

The possibility of increasing the LiCl dissolution rate can be realized by using acid solutions. However, keeping the SEI thin by dissolving LiCl is less attractive because the self-discharge rate is increased.

Acknowledgements

The author is indebted to J. Bilde-Søensen, Cliver Klitholm, Kjeld Larsen and Jørgen Lindbo for experimental assistance and the Danish Ministry of Energy for financial support.

References

1 A. N. Dey, *Thin Solid Films, 43* (1977) 131.

2 E. Peled, in J. P. Gabano (ed.), *Lithium Batteries*, Academic Press, London, 1983, p. 43.

3 M. Mogensen, in F. W. Poulsen, N. Hessel Andersen, K. Clausen, S. Skaarup and O. T. Sørensen (eds.), *Transport-structure Relations in Fast Ion and Mixed Conductors*, Risø National Laboratory, 1985, p. 233.

4 M. Mogensen, in *Proc. 9th Scandinavian Corrosion Congress*, Vol. 2, Korrosionscentralen, Copenhagen, 1983, p. 699.

5 M. Mogensen, *J. Power Sources, 14* (1985) 123.

6 J. P. Gabano, in E. B. Yeager (ed.), *Proc. Workshop on Lithium Non-aqueous Battery Electrochemistry*, Publication 80-7, The Electrochemical Society, Pennington, NJ, 1980, p. 98.

7 P. Schupp, *Z. Phys., 75* (1932) 84.

8 J. Errera, *Z. Elektrochem., 36* (1930) 818.